


Combination of *IFITM1* knockdown and radiotherapy inhibits the growth of oral cancer

Jie Yang^{1,†} | Lei Li^{1,2,†} | Yan Xi^{1,†} | Ruimei Sun¹ | Hu Wang¹ | Yanxin Ren¹ | Liufang Zhao¹ | Xiaoli Wang³ | Xiaojiang Li¹ 

¹Head and Neck Tumor Research Center, No. 3 Affiliated Hospital of Kunming Medical University (Tumor Hospital of Yunnan Province & Yunnan Cancer Center), Kunming, Yunnan, China

²The Affiliated Stomatological Hospital of Kunming Medical University, Kunming, Yunnan, China

³Radiation Therapy Center, No. 3 Affiliated Hospital of Kunming Medical University (Tumor Hospital of Yunnan Province & Yunnan Cancer Center), Kunming, Yunnan, China

Correspondence

Xiaoli Wang, Radiation Therapy Center, No. 3 Affiliated Hospital of Kunming Medical University (Tumor Hospital of Yunnan Province & Yunnan Cancer Center), No. 519 Kunzhou Road, Xishan District, Kunming, Yunnan, China
Email: season_202@163.com

and
Xiaojiang Li, Head and Neck Tumor Research Center, No. 3 Affiliated Hospital of Kunming Medical University (Tumor Hospital of Yunnan Province & Yunnan Cancer Center), No. 519 Kunzhou Road, Xishan District, Kunming, Yunnan, China
Email: hks51700@163.com

Funding information

National Natural Science Foundation of China Grant No. 81260312 to Xiaojiang Li

This research aimed to analyze the effect of *IFITM1* on the radioresistance of oral neoplasm. Using a multi-group heat map from GSE9716 analysis of the GEO database, *IFITM1* was determined to be a relevant radioresistance gene. The TCGA database was analyzed before the expression of *IFITM1* was analyzed. *IFITM1* expression was quantified by quantitative RT-PCR and immunohistochemistry in 19 paired oral neoplasm cases. The effects of time and dose of radiation on *IFITM1* expression level in CAL27 and TSCC1 cell lines were tested by quantitative RT-PCR. Oral neoplasm cells were transfected with siRNA after radiotherapy to disturb *IFITM1* expression. After this, the survival rates, cell apoptosis, caspase-3 viability, expression and γ -H2AX were detected using colony formation, flow cytometry, western blot and immunofluorescence, respectively. Western blot was used for STAT1/2/3/p21-related protein and phosphorylation changes. Finally, an in vivo nude mice tumor model was established to verify the effect of *IFITM1* on oral neoplasm cells radioresistance. Through microarray analysis, the head and neck neoplasm radioresistance-related gene *IFITM1* was found to be overexpressed. *IFITM1* overexpression was verified not only using the TCGA database but also in 19 paired cases of oral neoplasm tissues and cells. With increases of dose and time of radiation, the expression of *IFITM1* was increased in CAL27 and TSCC1 cell lines. Furthermore, si-*IFITM1* may restrain cell proliferation, DNA damage and cell apoptosis in oral neoplasm cell lines. Finally, pSTAT1/2/p21 was found to be upregulated while pSTAT3/p-p21 was downregulated due to *IFITM1* inhibition after radiotherapy. The evidence suggested that *IFITM1* in combination with radiotherapy can inhibit oral neoplasm cells.

KEYWORDS

IFITM1, oral cancer, oral neoplasm, radioresistance, radiotherapy

1 | INTRODUCTION

Oral neoplasm is the 6th most common form of cancer worldwide. Its incidence varies with geographic location, methods of detection

and ethnicity. However, a higher incidence of oral cancer is observed in South-East Asia, likely attributed to excessive use of tobacco. The ratio of males to females diagnosed with oral cancer in India has been reported to be 2:1, indicating a higher occurrence among males.¹ It is estimated that there are approximately 48 330 new cases and 9570 deaths due to oral cancer in the US annually. This

[†]These authors contributed equally to this work.

amounts to more than one fatality every hour due to oral cancer. Worldwide, approximately 300 000 cases and 145 000 deaths are reported annually.² Research dedicated to radiotherapy tolerance is on the rise, and the present research seeks to contribute to the treatment strategies of oral neoplasm using radiotherapy in combination with the inhibition of *IFITM1*.

Radiotherapy is regularly used in cancer treatment, with 40% to 60% of all cancer patients accepting the treatment.³ As an example, stereotactic ablative radiation therapy is one application of radiotherapy gaining popularity in the management of many disease types, including prostate cancer.⁴ Stereotactic radiosurgery involves delivering a single high dose over a small area while sparing the surrounding healthy tissue. Consequently, this treatment requires rigorous precision in immobilization and patient positioning.⁵ Resistance to chemotherapy remains problematic. Up to one-third of LABC are resistant to chemotherapy and/or hormone therapy and remain inoperable. It is possible to treat such patients with radiotherapy to reduce tumor burden and allow resection. At the Brazilian National Cancer Institute many patients are diagnosed when the disease is locally advanced, and a significant proportion thus have a poor response to neoadjuvant chemotherapy regimens involving anthracyclines ± taxanes ± trastuzumab. Therefore, other therapies are required, such as radiotherapy, to reduce the tumor burden with the goal of surgical resection.⁶ Radiotherapy is a crucial method commonly used in cancer management. Hence, this study was designed to apply radiotherapy in oral neoplasm.

Interferon-induced transmembrane protein 1 (*IFITM1*) is a member of the IFN-inducible transmembrane protein family and of the multimeric complex involved in cell adhesion signals and transduction of anti-proliferation.⁷ Following its recognition in hologenome expression analysis of tumor cells, the effects of *IFITM1* began to be widely studied, which accordingly led to the recognition of its role in drug response and cell invasion. More recently, a set of studies have illustrated correlations between overexpression of *IFITM1* and the progression of cancers in diverse tissues, including ovarian cancer, head and neck cancer, colorectal cancer, gastric cancer, lymphoma, leukemia and cervical squamous cell carcinoma.⁸ Hence, it is very likely that *IFITM1* may also hold hitherto undiscovered value elsewhere. Thus, the present study combines *IFITM1* and radiotherapy to make new headway in the treatment of oral neoplasm.

This research contains extensive experiments, including quantitative RT-PCR (qRT-PCR), immunohistochemistry, colony formation, flow cytometry, western blot, immunofluorescence and a nude mice tumor model, to verify the effects of radiotherapy and the expression of *IFITM1* with change of time and dose in oral neoplasm, to observe cell proliferation and cell apoptosis rates, to detect caspase-3 viability, expression and γ -H2AX, to measure the STAT1/2/3/p21-related protein and phosphorylation changes and to demonstrate the effect of *IFITM1* on oral neoplasm cells radioresistance. The results indicate that inhibition of *IFITM1* in combination with radiotherapy could, indeed, inhibit oral neoplasm cells; therefore, this research may lead to some improvements in the treatment of oral neoplasm.

2 | MATERIALS AND METHODS

2.1 | Patients and samples

The study included 19 cancer tissues and adjacent tissues before radiotherapy and 19 cancer tissue samples after radiotherapy (three cases with radiotherapy 15 Gy, 8 cases with radiotherapy 18 Gy, eight cases with radiotherapy 21 Gy) from patients with oral neoplasm at the No. 3 Affiliated Hospital of Kunming Medical University. All cancer tissues and their adjacent tissues from patients with oral neoplasm who had not received radiotherapy or other cancer-related therapies before surgery were immediately placed in liquid nitrogen and preserved in a freezer at -80°C until use. All specimens were pathologically verified. This study was authorized by the Ethics Committee of the No. 3 Affiliated Hospital of Kunming Medical University with all patients consenting.

2.2 | Cell lines and cell cultures

KB (TCHu 73) oral epidermoid carcinoma cells were purchased from the Chinese Academy of Sciences Cell Bank (Shanghai, China), and maintained in minimum essential medium (MEM) containing NaHCO_3 1.5 g/L, sodium pyruvate 0.11 g/L and 10% FBS (Life Technologies, Grand Island, NY, USA). BeNa Culture Collection provided human tongue squamous cell carcinoma cell line CAL27 (BNCC102194), oral squamous cell carcinoma cell line TSCC1 (BNCC102211) and normal oral epithelial cell line HOEC (BNCC340217). CAL27 was sustained in DMEM with 10% FBS while MEM with 10% FBS was utilized to support TSCC1. HOEC was maintained in DMEM with 90% high glucose and 10% FBS in 5% CO_2 and 95% air at 37°C .

2.3 | Cell transfection

BLOCK-iTTM RNAi Designer (Invitrogen, Carlsbad, CA, USA) was used to design the interfering nucleotide sequence. Meanwhile, the unrelated nucleic acid sequences of the same base number, designed and synthesized in the same way, served as a negative control (related sequences are listed in Table 1). They were then transformed to competent cells for expansion. Positive clones were picked and the recombinant plasmid was extracted and sequenced. Cells were transfected

TABLE 1 siRNA sequences designed by BLOCK-iT RNAi designer

Gene	Sequence (5'-3')
SiIFITM1	TGGTATTCCGGCTCTGTGACAGTCTA
SiNC	TGGGCTTCTCGGTGTGACATATCTA

TABLE 2 Primers for quantitative RT-PCR

Gene name	Primer sequence (5'-3')
IFITM1 forward	TCGCCTACTCCGTGAAGTCTA
IFITM1 reverse	TGTACAGAGCCGAATACCAG
GAPDH forward	TATAAATTGAGCCCGCAGCC
GAPDH reverse	TACGACCAAATCCGTTGACTC

using Lipofectamine 2000 (Invitrogen) at a concentration of 50 nmol/L following the manufacturer's instructions. Transfection efficiency was observed after the cells were cultured for 24 and 48 hours.

2.4 | Immunohistochemistry

Paraffin-embedded pathological sections were deparaffinized and rehydrated. Antigens were then retrieved using PBS containing 0.1% trypsin at 37°C for 30 minutes. Before antibody reactions, endogenous peroxidase was inactivated with 5 minutes 3% hydrogen peroxide incubation at room temperature followed by rinsing with PBS. Samples were incubated with 5% BSA for 10 minutes and primary antibodies *IFITM1* (ab224063, 1:200, Abcam, Cambridge, MA, USA) were diluted and added to slides. Secondary antibody horseradish enzyme-labeled goat anti-rabbit IgG was applied to each slide, which were then incubated for 30 minutes and washed three times with PBS. Finally, each specimen-containing slide was developed using chromogen DAB for 20 seconds, and counterstained with hematoxylin for 1 minute. After staining was completed, slides were sealed and observed by two independent reviewers under a microscope. The expression level of *IFITM1* was evaluated by total score, which was taken as dyeing intensity score plus dyeing range score (the ratio of positive stained cells in the cell membrane and cytoplasm).

2.5 | Extraction of RNA and quantitative RT-PCR

RNA primers (primers used are exhibited in Table 2) were designed and colligated by Sangon Biotech (Shanghai, China). The total RNA of cells was extracted using Trizol. Next, the concentration and purity of the total RNA were measured in the same way. Total RNA were reverse-transcribed into cRNA using a First Strand Synthesis Kit (Thermo Fisher Scientific, Waltham, MA, USA) according to manufacturer guidelines. First strand cDNA was stored at -20°C before real-time PCR, which subjected cDNA to the ABI PRISM 7000 Sequence Detection System using Maxima SYBR Green qPCR Master Mix (2×) (Thermo Fisher Scientific). The samples were amplified using β -actin as internal control and reaction conditions were as follows: original denaturation at 95°C for 5 minutes with another extension at 72°C for 5 minutes, followed by 40 cycles of 95°C for 15 seconds and 60°C for 30 seconds. After all of this was completed, results were analyzed using Step One Software v2.1 in $2^{-\Delta\Delta C_t}$, which analyzed the gene relative expression level.

2.6 | Radiotherapy

Cells and mice were irradiated at doses 2, 4, 6 and 8 Gy/min with 250 kV X-rays (Philips RT250, Kimtron Medical) at a distance of approximately 50 cm from the radiation source.

2.7 | Colony formation and survival analysis

Adherent cells were digested with trypsin and released into 96-well plates, at 500 cells per well. Single cell suspension was transferred

to 10-mL tubes. Into these tubes, 3 mL $2 \times$ RPMI + 10% FCS and 3 mL 0.7% agarose were added and mixed by gentle swirling. Finally, 1.5 mL of the mixture was added to three replicate plates for incubation at 37°C in a humidified incubator. Cells were exposed to 8-Gy radiation every 3 days. Crystal violet was then applied to stain cells for 10 minutes. The staining fluid was removed and cells were air-dried. ColCount colony counter (Oxford Optronix, Abingdon, UK) was utilized to count colony numbers. Plating efficiency (PE) was calculated as follows: PE = number of cloning/number of vaccination, and this was compared with the negative control group. Survival rate (SF) was calculated as follows: SF = number of cloning/number of vaccination*PE.

2.8 | Cell apoptosis assay

Cell apoptosis was analyzed using an Annexin V Apoptosis Detection Kit (Beyotime, Shanghai, China). Medium was placed into a constant temperature oven (37°C) with 5% CO₂ after transfection and cells were exposed to 8-Gy radiation. Oral neoplasm cells were collected after 24 hours. The cells were placed in EP tubes after centrifugation with the number of cells in each tube being greater than 1×10^6 . Annexin V-FITC and PI were then added. Cells were put on ice in the dark after gentle shaking. PBS was then used to wash cells twice and disposed of by centrifugation (167.7 g) for 5 minutes at room temperature. Cells were resuspended in 500 μ L after the removal of suspension. Finally, cells were tested using FCM.

2.9 | Caspase-3 activity assay

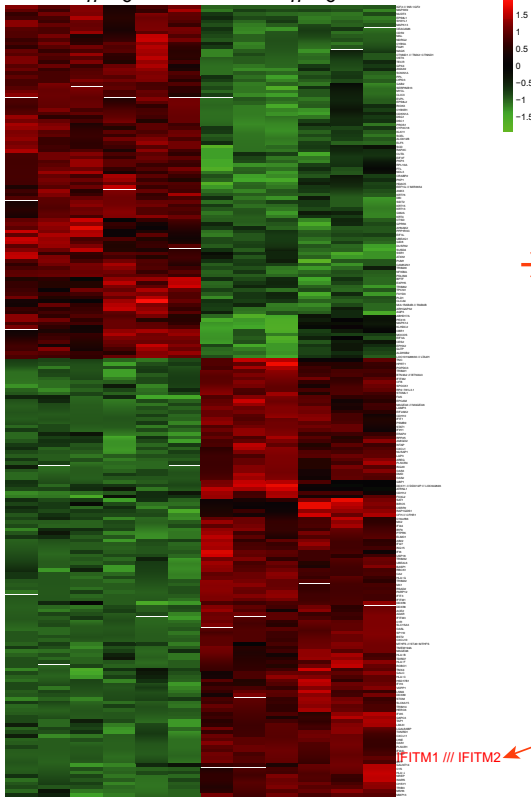
PNA was diluted to 0, 10, 20, 50, 100 and 200 μ mol/L, having been supplied by caspase-3 (Beyotime). The standard curve was plotted while taking PNA concentration as abscissa and optical density,

TABLE 3 Antibodies used for western blot, immunohistochemical staining and immunofluorescent staining

Protein	Catalog	Dilution	Company
IFITM1	ab224063	1/100	Abcam
Cleaved caspase3	#9661	1/500	CST
γ H2AX	ab2893	1/500	Abcam
GAPDH	ab181602	1/10 000	Abcam
p-STAT1(S727)	ab109461	1/5000	Abcam
STAT1	ab31369	1/1000	Abcam
p-STAT2(Y690)	ab53132	1/3000	Abcam
STAT2	ab134192	1/2000	Abcam
p-STAT3(S727)	ab32143	1/1000	Abcam
STAT3	ab32500	1/2000	Abcam
p-p21(T145)	ab47300	1/200	Abcam
p21	ab109520	1/2000	Abcam
IgG-HRP	ab8227	1/2000	Abcam
IgG-Cy3	ab6939	1/500	Abcam

p means the location of phosphorylated protein.

(A) Radiosensitive tumor *n* = 6 Radioresistant tumor *n* = 6



(B) Radioresistant tumor Radiosensitive tumor
0 h 5 h 24 h 0 h 5 h 24 h

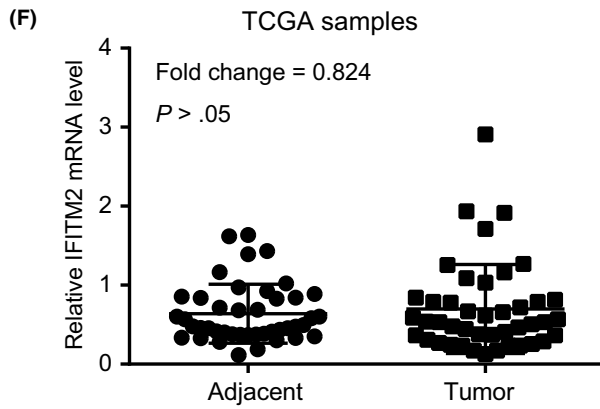
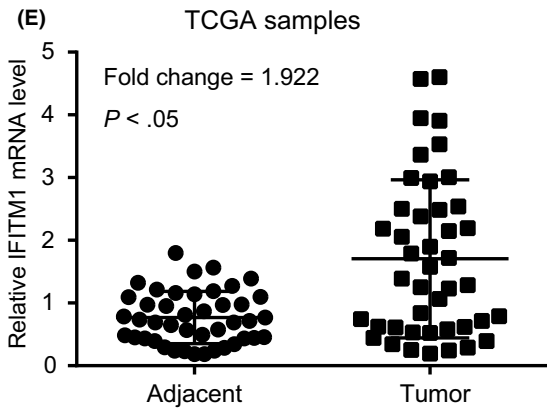
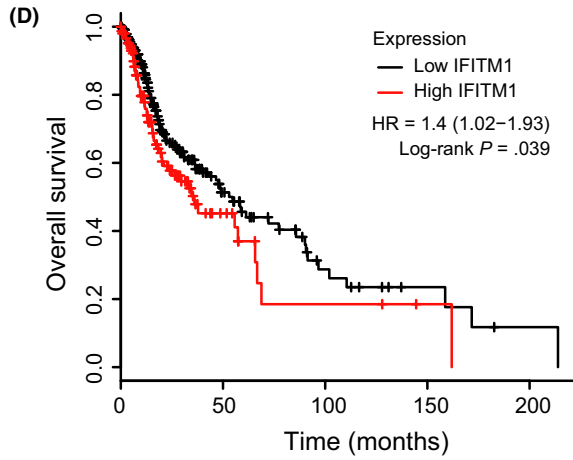
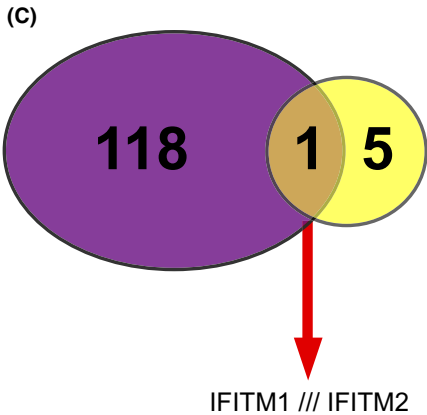
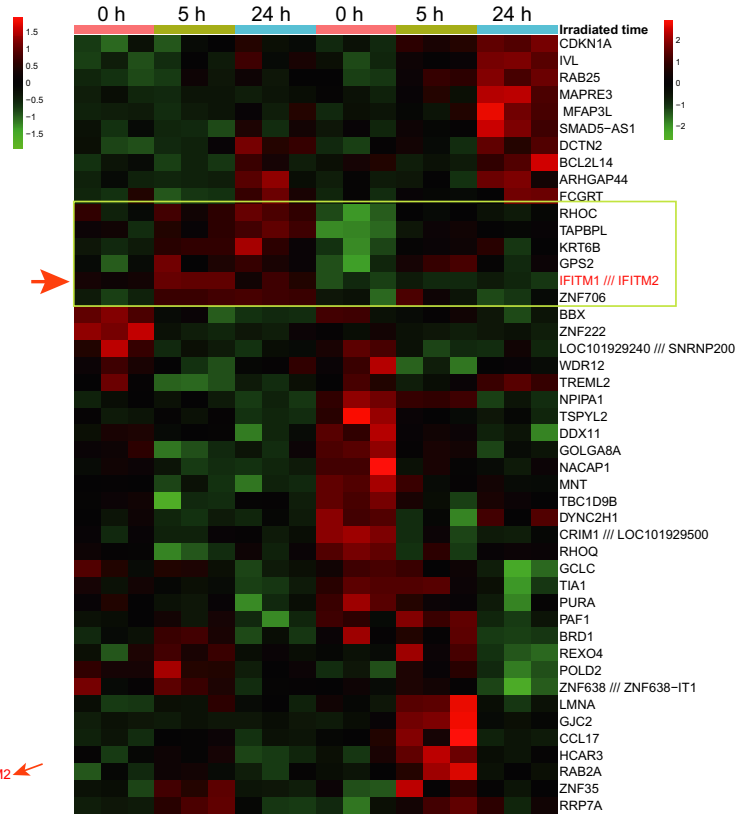


FIGURE 1 Screening of Radiation-Related Gene *IFITM1* in Head and Neck Tumor Cells. A, Twelve samples obtained from GSE9716 and were divided into two groups: radiosensitive-tumor, radioresistant-tumor, each group with six samples. The heat map showed the differential genes with screening conditions of $P < 0.00001$ and $|\log_2(\text{Fold Change})| > 2$. The red arrow indicates higher expressed genes *IFITM1* and *IFITM2* in radioresistant groups when compared with radiosensitive groups. B, 18 samples obtained from GSE9716 were divided into six groups: radioresistant-untreated, radioresistant-5 h-post-IR, radioresistant-24 h-post-IR, radiosensitive-untreated, radiosensitive-5 h-post-IR and radiosensitive-24 h-post-IR (each group had three samples). The heatmap shows the differential genes with screening conditions of $P < 0.001$ and $|\log_2(\text{FoldChange})| > 1$. The yellow box indicates that genes are highly expressed as the radiation time increases in radioresistant groups but expressed at low levels in radiosensitive groups, and the red arrow shows the most radioresistant-associated genes, *IFITM1* and *IFITM2*. C, Venn diagram: The intersection of 119 highly expressed genes in radioresistant tumors and six radioresistant-associated differentially expressed genes was *IFITM1/IFITM2*. D, Prognosis KM curve: low *IFITM1* expression contributes to the prognosis of patients with head and neck squamous cell carcinoma based on the TCGA database ($P = 0.039$). E-F, Analysis of differences in levels of *IFITM1* and *IFITM2* between normal tissue samples and tumor samples using the TCGA database. The expression of *IFITM1* in tumors was 1.922 times than that in the adjacent tissues and $*P < 0.05$, which indicates that there were significant differences. However, the expression of *IFITM2* in tumors was 0.824 times than that in the adjacent tissues and $P > 0.05$, which indicates no significant difference

detected using a microplate reader for the ordinate. The medium was placed in a constant temperature oven (at 37°C) with 5% CO₂ after transfection and cells were exposed to 8-Gy radiation. Oral neoplasm cells were collected after 24 hours and the concentration of cells was regulated to 2×10^6 cells/group. Cells were then separated by centrifugation (167.7 g) at 4°C for 5 minutes and suspension was removed. Cells were washed twice with PBS. Lysis buffer was then added. Cells were stemmed with ice-water for 15 minutes after resuspension. Then, cells were separated by centrifugation (14 000 g) at 4°C for 15 minutes; 10 µL suspension was placed into a precool EP tube; 80 µL detection buffer and 10 µL Ac-DEVD-PNA was added, mixed well and the resultant suspension incubated at 37°C overnight. Optical density was detected using a microplate reader at 490 nm. Finally, the expression of caspase-3 protein was verified by western blot.

2.10 | γ H2AX detected by immunofluorescence assay

Next, 1×10^4 cells were seeded in a 24-well plate containing slides. After different transfection treatments, medium was placed into a constant temperature oven at 37°C with 5% CO₂. Cells were exposed to 8-Gy radiation. After 24 hours, medium was washed three times with pre-warmed 1× PBS for 10 minutes each. Air-dried slides were fixed with 4% formaldehyde in TBS for 15-20 minutes at room temperature and washed three times with 1× PBS for 10 minutes each. Cells were then permeabilized with 0.2% Triton X-100 for 4 minutes and washed three times with 1× PBS for 10 minutes each. These cells were then blocked in 5% BSA at room temperature for 30 minutes. γ -H2AX primary antibody (Abcam) was added at 4°C overnight. Cells were washed three times with 1× PBS for 10 minutes each. Next, Cy3 fluorescently labeled secondary antibody (Abcam) was added for 1 hour at room temperature in darkness. Cells were then washed as before. After soaking in Hoechst's solvent for 15 minutes, the plate was sealed with 95% glycerol. Finally, cells were observed under a fluorescence microscope for photographing, at randomly selected multiple fields of view (800) for the counting of foci. Each experiment was repeated three times.

2.11 | Western blot

RIPA lysis buffer was used to lyse cells and extract total protein. The BCA method was adopted to measure the total protein concentration in each group. SDS-PAGE gels were prepared. Protein was electrophoretically transferred to a polyvinylidene difluoride (PVDF) membrane. Next, 5% BSA was applied to immersed PVDF membrane for 30 m at room temperature. Meanwhile, primary antibody (detail information provided in Table 3), diluted with TBST at 5% BSA, was added at 4°C overnight. After this, PVDF membrane was washed with TBST three times and incubated in horseradish enzyme-labeled secondary antibody (Abcam) with 5% BSA for approximately 1 hour at room temperature. Following this, it was washed by TBST three times once again. The PVDF membrane was then exposed, developed, cleaned and fixed. Image J was used to achieve semi-quantitative analysis of the cumulative optical density of the band and to calculate the relative expression of each protein of interest.

2.12 | Mouse allotransplantation assay

The 24 4-6-week-old Balb/c male mice used for this study were divided equally into four groups. All mice were purchased from the No. 3 Affiliated Hospital of Kunming Medical University and all animal experiments were informed and carried out in accordance with protocols approved by the same body. To establish a tumor model, CAL27 was transfected with siNC or si-*IFITM1*, respectively, before irradiation. The cells were irradiated with a dose of 8 Gy/min before being injected into the mice. Mice were placed in lead shielding jigs and exposed tumors received 8 Gy dose irradiation every 3 days using a 250 kVp orthovoltage therapeutic X-ray machine (Philips, Andover, MA). Moreover, 10^6 CAL27 cells transfected with siRNA were injected into the peritumoral area every 5 days for mice in each group. Tumors were measured every week in three dimensions using vernier calipers. The tumor growth curve was calculated and plotted using the formula $V = 1/2 \times \text{length} \times \text{width}^2$. After day 30, mice were killed and tumor tissues were isolated. Samples were ground using liquid nitrogen and total RNA was extracted from tumors.

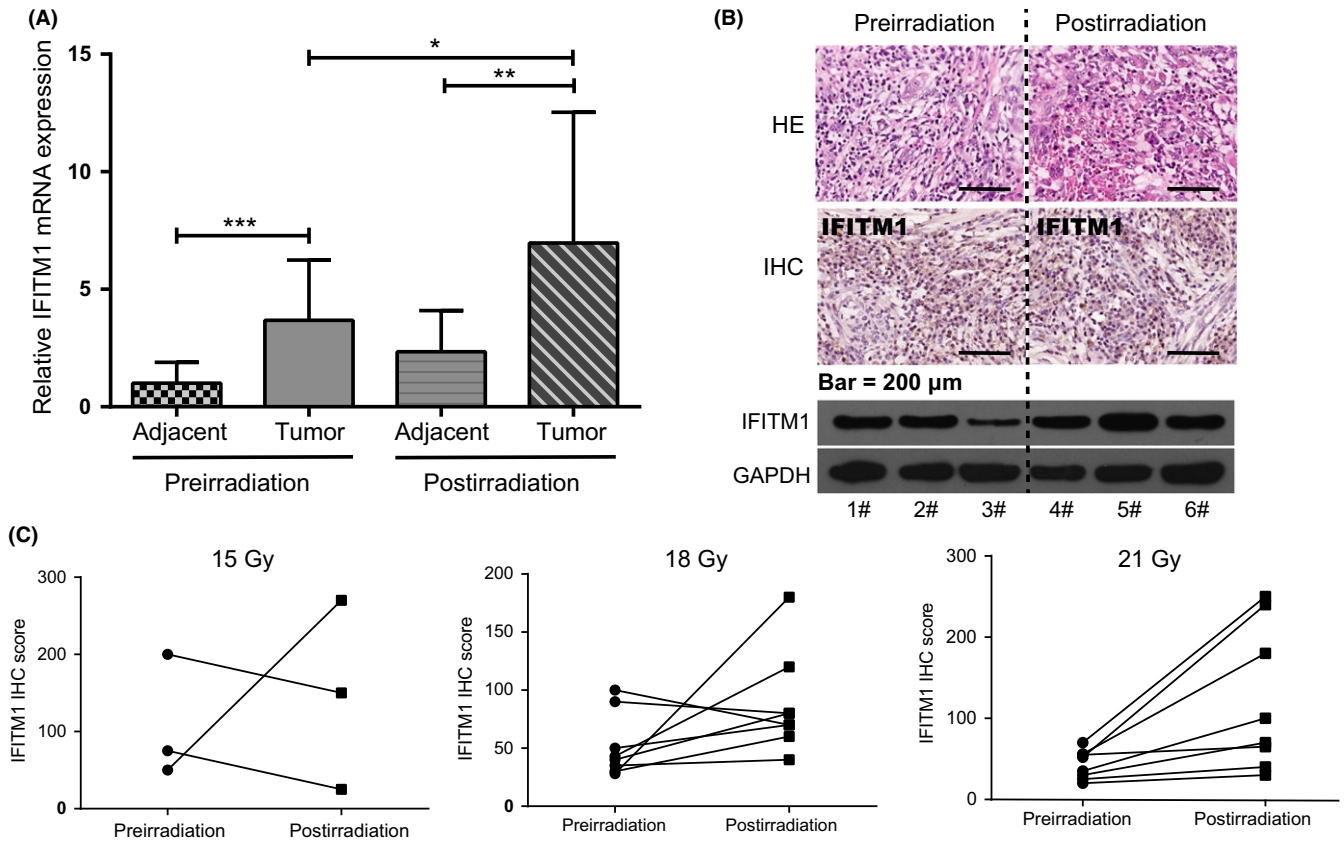


FIGURE 2 *IFITM1* Was Highly Expressed in Oral Neoplasm Tissues and Cells. A, The high mRNA expression of *IFITM1*, which significantly increased after radiation, was measured by quantitative RT-PCR. * $P < 0.05$ meant that there was significant difference. B, Immunohistochemistry demonstrated that *IFITM1* protein increased after radiotherapy in oral neoplasm tissues. C, Immunohistochemical score of *IFITM1* protein after radiation at 15, 18 and 21 Gy in oral neoplasm tissues. D, *IFITM1* mRNA expression, which was evaluated using qRT-PCR in oral neoplasm cell lines KB (TCHu 73), CAL27 (BNCC102194) and TSCC1 (BNCC 102211), was significantly higher than in normal oral epithelial cells, HOEC (BNCC340217). * $P < 0.05$ meant that there was significant difference compared to HOEC

Finally, the level of *IFITM1* mRNA expression was evaluated using qRT-PCR for each group.

2.13 | Microarray

GSE9716 containing 38 samples (from GSM245389 to GSM245426) was used to detect differentially-expressed genes in radioresistant and radiosensitive human head and neck tumors before and after irradiation. In this study, the first 30 samples of GSM245389-GSM245418 were selected for analysis using GPL96 (Affymetrix Human Genome U133A Array). Among these, 12 samples of GSM245389-GSM245400 were divided into four groups: radioresistant tumor-untreated, radioresistant tumor-irradiated, radiosensitive tumor-untreated and radiosensitive tumor-irradiated (each group contained three samples). The remaining 18 samples were divided into six groups: radioresistant tumor-untreated, radiosensitive tumor-untreated, radioresistant tumor-5 hour post-IR, radiosensitive tumor-5 hours post-IR, radioresistant tumor-24 hours post-IR and radiosensitive tumor-24 hour post-IR (each group contained three samples). The heatmap was generated by R language standardization and multi-factor analysis of variance assay. Differentially expressed

genes were screened with limitations of $P < 0.00001$ and $|\log(\text{Fold-Change})| > 2$ (Figure 1A), and $P < 0.001$ and $|\log(\text{Fold-Change})| > 1$ (Figure 1A).

2.14 | Statistical analysis

GraphPad Prism version 6.0 (GraphPad Software, La Jolla, CA, USA) was used to perform statistical analysis. An unpaired student's t test was used to examine differences between groups. Differences among the groups of samples were assessed by one-way ANOVA. $P < 0.05$ was considered statistically significant.

3 | RESULTS

3.1 | Screening of radiation-related gene *IFITM1* in head and neck tumor cells

Four groups from GSE9716 were selected for microarray analysis: radiosensitive-untreated, radiosensitive-irradiated, radioresistant-irradiated and radioresistant-untreated. Three samples in each group were analyzed via multi-factor ANOVA. Differential genes were

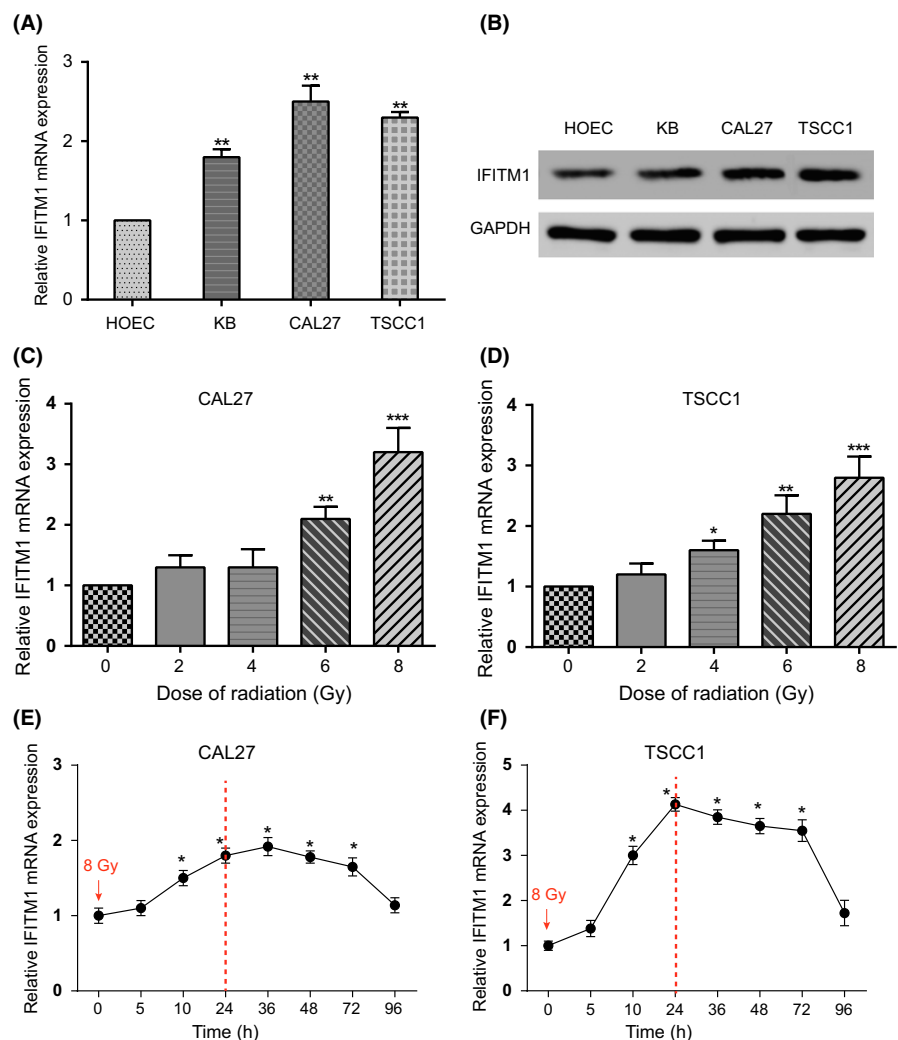
obtained and a heat map was composed with $P < 0.00001$ and $|\log(\text{FoldChange})| > 2$ as the screening condition, which showed 119 genes highly expressed in the radioresistant group (Figure 1A). Following this, 18 samples of GSM245400-GSM245418 from GSE9716 were divided into six groups: radioresistant-untreated, radioresistant-5 hour-post-IR, radioresistant-24 hour-post-IR, radiosensitive-untreated, radiosensitive-5 hour-post-IR and radiosensitive-24 hour-post-IR. Three samples in each group were analyzed by multi-factor ANOVA. In total, 46 differential genes were obtained with the restriction of $P < 0.001$ and $|\log(\text{FoldChange})| > 1$ (Figure 1B). The yellow box illustrates the different genes at 0, 5 and 24 hours radiotherapy time, which were found to be increased in radioresistant but decreased in radiosensitive groups. To explore the underlying genes involved in radioresistance, the 119 highly expressed genes in the radioresistant group, whether irradiated or untreated, and six highly expressed genes (the yellow box) in the radioresistant group after irradiation for 5 and 24 hours were intersected, and most radioresistant associated genes (*IFITM1/IFITM2*) were found (Figure 1C). The expression levels of *IFITM1* and *IFITM2* are shown in Figure 1B. The gene expression level was gradually increased with the corresponding increase of radiotherapy time in radioresistant cells,

while the gene expression level was always weaker in radiosensitive cells, further lending weight to the conclusion that there exists a connection between the radiotherapy tolerance of head and neck tumor cells and *IFITM1* and *IFITM2*. Moreover, patients were analyzed for prognosis using the TCGA database and the results showed that patients with higher *IFITM1* expression saw a worse prognosis ($P < 0.05$) (Figure 1D), which further suggests that *IFITM1* might be related to radiotherapy tolerance. Paired-differentiated analysis of cancer tissues and paracancerous tissues was applied to head and neck squamous cell carcinoma (HNSC) tumor samples using the TCGA database, which clarified that the fold change of *IFITM1* was 1.922 (Figure 1E) while that of *IFITM2* was 0.824 (Figure 1F). Hence, *IFITM1* was deemed to the closest irradiated gene in HNSC.

3.2 | *IFITM1* overexpression in oral neoplasm cells and tissues

The expression of *IFITM1* was analyzed in 19 cases of oral neoplasm and the corresponding paracancerous specimen before and after radiotherapy. *IFITM1* expression level in cancer tissues was found to be higher than that in paracancerous tissues, and *IFITM1* expression

FIGURE 3 *IFITM1* Expression Was Upregulated With the Increase of Time and Dose of Radiation. (A, B) The expression of *IFITM1* increased gradually in CAL27 cells and TSCC1 cells. $**P < 0.01$ meant that there was significant difference. (C, D) The expression of *IFITM1* increased gradually in CAL27 cells and TSCC1 cells treated with different doses, ranging from 0 Gy, 2 Gy, 4 Gy, 6 Gy and 8 Gy. Moreover, *IFITM1* expression was highest at 8 Gy. $***P < 0.001$ meant that there was significant difference compared to 0 Gy. (E, F) At 8 Gy irradiation doses, *IFITM1* expression gradually increased in CAL27 cells and TSCC1 cells at different times: 0 h, 5 h, 10 h and 24 h. *IFITM1* expression was highest at 24 h in TSCC1 cells. Significant difference occurred on the basis of $**P < 0.01$ compared to 0 h.



in cancer tissues after radiotherapy was significantly higher than before radiotherapy ($P < 0.05$, Figure 2A). H&E staining and immunohistochemistry showed that IFITM1 was mainly expressed in cytoplasm and membrane, while western blot of three 21-Gy patients' tissues showed higher expression of IFITM1 in post-irradiation groups when compared with pre-irradiation groups ($P < 0.05$, Figure 2B). The scores of immunohistochemistry in different tissue samples before and after radiotherapy showed that the irradiation intensity of three samples was 15 Gy (one case increased), the irradiation intensity of eight samples was 18 Gy (five cases increased) and the irradiation intensity of eight samples was 21 Gy (five cases increased). Overall, the results illustrated that IFITM1 expression was significantly increased in 11 cases ($P < 0.05$, Figure 2C).

3.3 | IFITM1 expression was upregulated with the increase of time and dose of radiation

The analysis of IFITM1 expression level in diverse cell lines showed that the IFITM1 mRNA and protein expressions in oral neoplasm cell lines KB (TCHu 73), CAL27 (BNCC102194) and TSCC1 (BNCC102211) were higher than in HOEC (BNCC340217) (all $P < 0.05$, Figure 3A,B). Compared with HOEC and KB, CAL27 and TSCC1 both had higher IFITM1 expression, which was the motivation behind their selection for the following experiments. The increase of IFITM1 mRNA expression was verified by qRT-PCR assay in CAL27 cells and TSCC1 cells with differing doses of radiation; namely, 0, 2, 4, 6 and 8 Gy. Significant statistical differences were found above 6 Gy ($P < 0.05$, Figure 3C,D). Similarly, CAL27 cells and TSCC1 cells were selected to receive 8-Gy radiation IFITM1 level was measured after radiation of different durations, including 0, 5, 10, 24, 36, 48, 72 and 96 hours ($P < 0.05$, Figure 3E,F). The

straight-line graphs showed that IFITM1 expression peaked after radiation for 24–36 hours and the higher expression was sustained for 3 days until it sharply declined on the 4th day.

3.4 | IFITM1 expression inhibited decreased cell viability and promoted cell apoptosis

To further verify the relationship between IFITM1 and radiosensitivity of oral neoplasm, the expression of IFITM1 was disturbed with specific siRNA in CAL27 cells and TSCC1 cells. siRNA of IFITM1 significantly reduced IFITM1 compared to the control group siNC before and after irradiation in two cell lines ($P < 0.05$, Figure 4A,B). CCK8 assay was used to test cell viability after the radiotherapy dose was gradually increased, and the results showed that the cell survival rate gradually decreased after downregulating IFITM1 with significant statistical differences at doses of 6 and 8 Gy ($P < 0.05$, Figure 4C,D). The colony formations of CAL27 and TSCC1 cell lines are shown in Figure 5A,B at 8-Gy doses. The si-IFITM1 group was found to have the least number of colonies ($P < 0.05$). Similarly, cells were significantly apoptotic after inhibiting the expression of IFITM1 at 8-Gy doses ($P < 0.05$, Figure 5C,D).

3.5 | IFITM1 expression inhibited upgraded caspase-3 vitality and expression, and resulted in DNA damage

Cell apoptosis and protein γ -H2AX expression were evaluated after DNA damage by caspase-3 activity assay and immunofluorescence assay, respectively, to further demonstrate that IFITM1 expression affected radiotherapy-induced apoptosis, thereby affecting the radioresistance of oral neoplasm cells. The results indicated that caspase-3 vitality and expression of the si-IFITM1 group were significantly

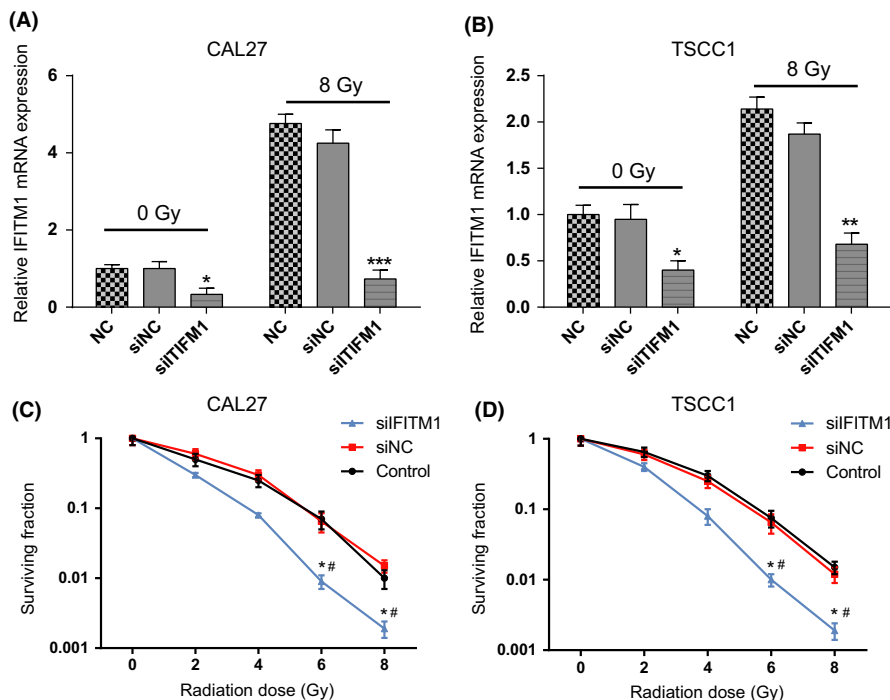


FIGURE 4 Inhibition of IFITM1 promoted the effect of radiation on cell surviving. (A, B) Transfection efficiency validation of siRNAs, specific siRNAs for IFITM1 were able to down-regulate IFITM1 mRNA levels in CAL27 cells and TSCC1 cells with or without irradiation. Data were represented with mean and SD ($n = 3$), $*P < 0.05$ compared to siNC group. (C, D) The survival rates of the si-IFITM1 group were decreased in CAL27 cells and TSCC1 cells at 8 Gy radiation. Survival rates were detected using CCK8. $*P < 0.05$ compared to control group while $\#P < 0.05$ compared to siNC group. Data were represented with mean and SD ($n = 3$)

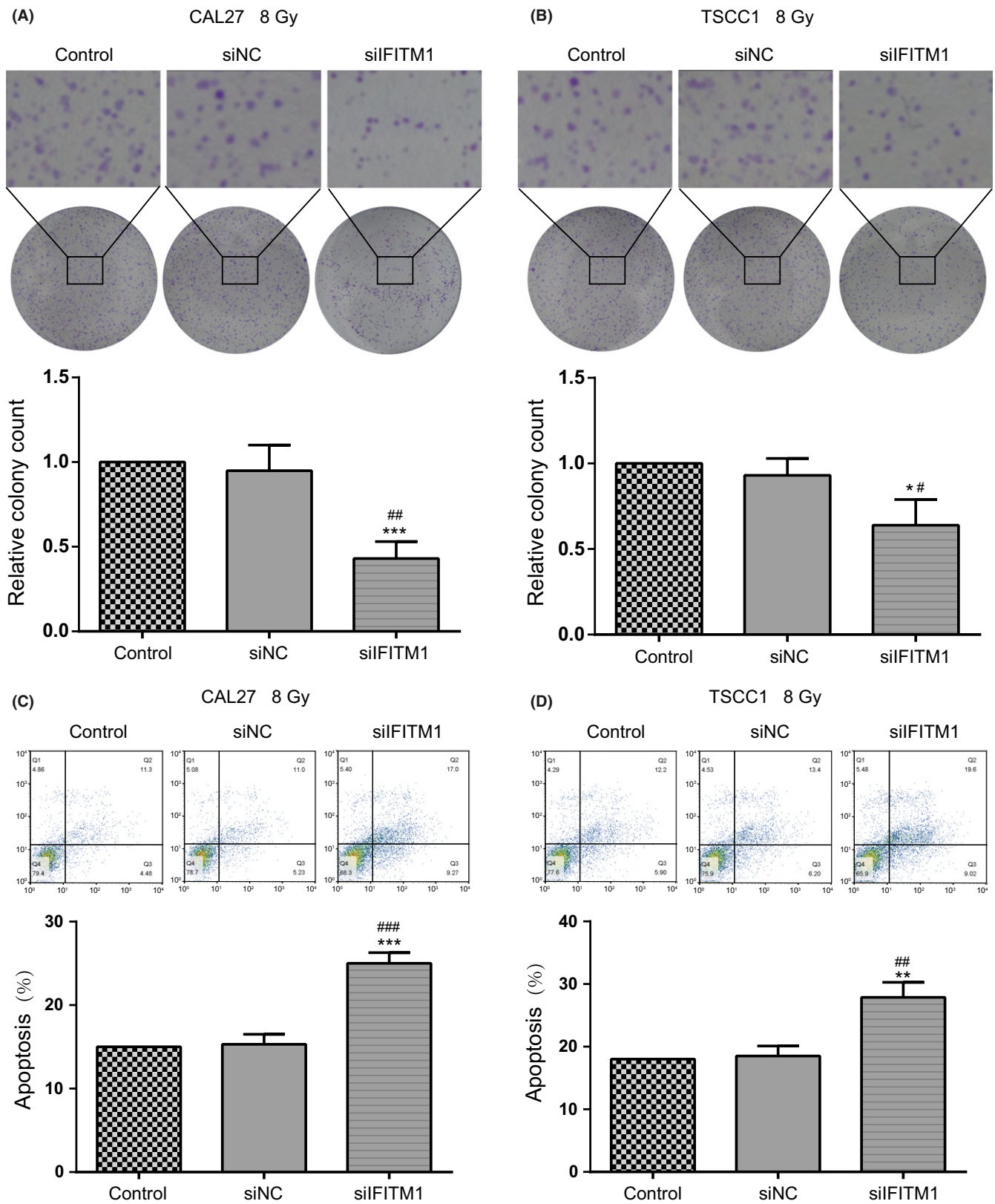


FIGURE 5 Inhibition of IFITM1 could decrease cell viability and promote cell apoptosis(A–B) Clone formation assay detected a decrease of si-IFITM1 group in colony formation. * $P < 0.05$ meant that there was significant difference compared with control group while # $P < 0.05$ meant that there stood significant difference compared to siNC group. (C–D) Flow cytometry showed increased apoptosis in si-IFITM1 group. ** $P < 0.01$ compared to control group while ### $P < 0.01$ compared to siNC group. Data were represented with mean and SD ($n = 3$).

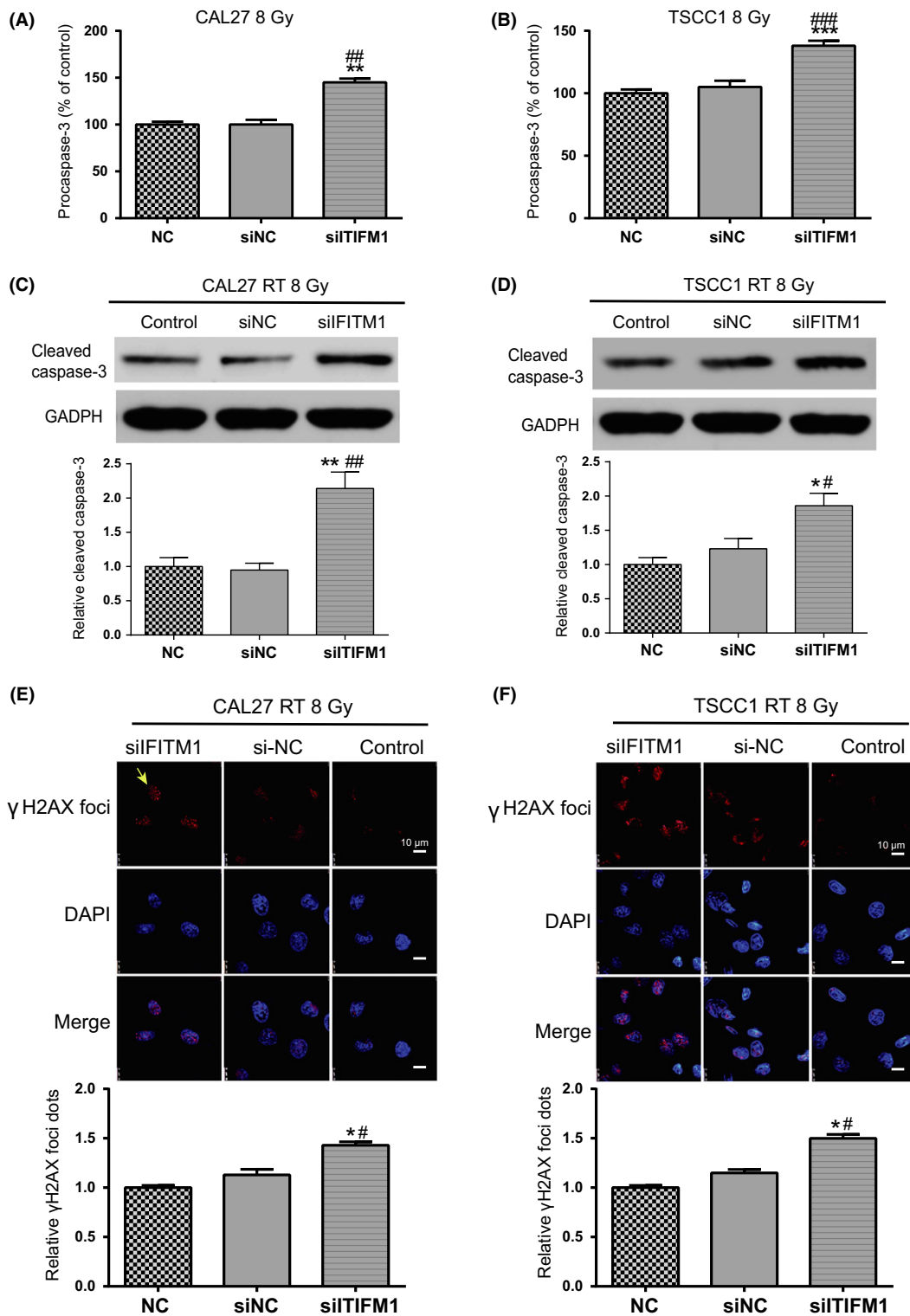


FIGURE 6 IFITM1 inhibition upgraded caspase-3 vitality and expression and DNA damage(A–B) The density ratios of the activation of procaspase-3 were first calculated in CAL27 and TSCC1 cells. The changes were expressed as the percentage of controls. Significant statistical difference occurred on the basis of $**P < 0.01$ compared to control group while $^{##}P < 0.01$ compared to siNC group. (C–D) Representative blots of caspase-3 protein in oral neoplasm cells compared to GADPH. $**P < 0.01$ compared to control group; $^{##}P < 0.01$ compared to siNC group. (E–F) γ -H2AX was stained with secondary antibody (red) and its nuclear counter stain was DAPI (blue). $*P < 0.05$ meant that there lay significant statistical difference compared to control group while $^{#}P < 0.05$ compared to siNC group. Data were represented with mean and SD (n = 3).

increased in CAL27 and TSCC1 cell lines ($P < 0.05$, Figure 6A-D). The formation of γ -H2AX is related to DNA double-strand breaks (DSB). There existed a linear positive correlation between the number of γ -H2AX foci and the number of DSB, and, hence, the formation of a focal spot of γ -H2AX molecules suggests DSB production. The outcomes showed that the γ -H2AX foci number in the si-*IFITM1* group increased significantly ($P < 0.05$, Figure 6E,F). The above results showed that, after inhibiting the expression of *IFITM1*, the apoptosis of oral neoplasm cells was significant.

3.6 | *IFITM1* affects radiation tolerance of oral cancer cells via STAT1/2/3/p21

STAT proteins are a class of important signal transducers and activators of transcription. After STAT is phosphorylated, it undergoes polymerization to become an activated transcriptional activator in the form of a homodimer or heterodimer which enters the nucleus to bind to specific sites in the target gene promoter sequence, facilitating its transcription. Meanwhile, in the literature, a close relationship between *IFITM1* and STAT1/2/3/p21 is demonstrated.⁹⁻¹¹

Changes in various proteins were measured using STAT1/2/3/p21 total protein antibody and its phosphorylation antibody, respectively, to observe the STAT1/2/3/p21 expression after inhibiting *IFITM1* expression in drug-resistant oral neoplasm. This was intended to assess whether the signaling pathways in both oral neoplasm cells displayed a consistent trend while the STAT1/2/3 total protein showed little fluctuation, but the expression of p-STAT1/2/p21 was increased and the p-STAT3/p-p21 protein expression was reduced after *IFITM1* knockdown ($P < 0.05$, Figure 7).

3.7 | *IFITM1* in combination with radiation inhibited in vivo oral neoplasm tumorigenesis

We subcutaneously injected CAL27 cells transfected with siNC and si-*IFITM1*, respectively, which had been pre-treated with either 0 or 8 Gy radiation, to establish a mouse xenograft tumor model to investigate the effect of *IFITM1* expression on the radioresistance of oral neoplasm in vivo at day 0. After day 5, the corresponding mice were treated with varying doses of radiation daily (0 or 8 Gy) and the growth of tumor volume was measured and recorded every 5 days. The entire

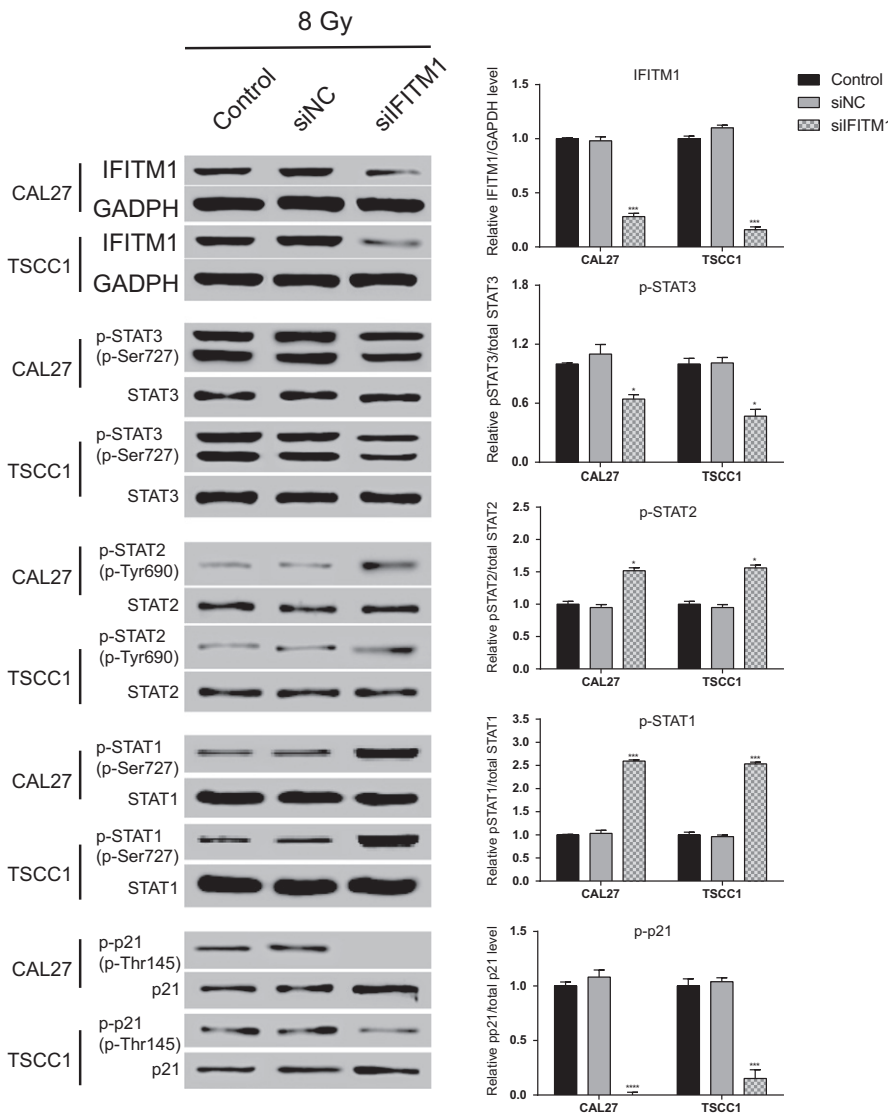


FIGURE 7 *IFITM1* affects radiation tolerance of oral cancer cells by regulating STAT1/2/3/p21. The primary antibodies to *IFITM1* and STAT1/2/3/p21 total protein were used to determine the amount of STAT1/2/3/p21 total protein. Phosphorylated protein was detected by phosphorylation of p-STAT1 (Ser727), p-STAT2 (Tyr690), p-STAT3 (Ser727) and p-p21 (Thr145). The remainder of the test was converted to the relative value of the NC group. Each experiment was repeated 3 times and the results were shown by SD and mean. Significant statistical difference occurred on the basis of ** $P < 0.01$ compared to control group while ## $P < 0.01$ compared to siNC group.

experimental design is simplified in Figure 8A. The *IFITM1* expression in four groups of isolated tumor cells was tested using RT-PCR, which showed that si-*IFITM1* successfully restrained *IFITM1* expression in the implanted tumor cells while *IFITM1* expression in the irradiated group was higher than in the non-irradiated group ($P < 0.05$, Figure 8B). By comparing the tumor volume of four groups of mice, this research found that radiation significantly inhibited CAL27 cells in in vivo tumorigenesis, but radiation treatment combined with si-*IFITM1* achieved better tumor suppression effects, and si-*IFITM1* alone could lead to some inhibition of tumor formation ($P < 0.05$, Figure 8C). In conclusion, this experiment illustrated that silencing *IFITM1* combined with radiotherapy could help to enhance radiosensitivity and achieve the best anti-tumor effect of the treatments studied.

4 | DISCUSSION

In summary, the first step of this research was to assess the radioresistance effect of interferon-induced transmembrane protein 1 (*IFITM1*). *IFITM1* expression and *IFITM1* IHC score were assessed in 19 oral neoplasm cases. This study also verified the expression of *IFITM1* and

si-*IFITM1* in CAL27 and TSCC1 cell lines. Of course, the *IFITM1* expression with different times and doses of radiation had to be tested in oral neoplasm cells. This research then ascertained cell proliferation, cell apoptosis, caspase-3 viability and expression, γ -H2AX, STAT1/2/3/p21-related protein and phosphorylation changes with the inhibition of *IFITM1* in combination with radiation in oral neoplasm cells. Finally, the effect of *IFITM1* on the radioresistance of oral neoplasm cells was verified in a nude mice tumor model. Thus, this research may offer valuable insights for the future treatment of oral tumors.

IFITM1 has been reported to be a tumor promoter in many papers, for its role in cervical squamous cell carcinoma as one example.¹² Its suppression blocked the proliferation and invasion of breast cancer⁹ and promoted the metastasis of human colorectal cancer.¹³ In this research, the overexpression of *IFITM1* was verified and the *IFITM1* overexpression prognosis was, indeed, worse. Hence, we speculated that *IFITM1* overexpression might be correlated with oral neoplasm. The expression of *IFITM1* has been found to be highly increased in cervical cancer, ovarian cancer and esophageal cancer.^{12,14,15} Therefore, recent research posits that *IFITM1* hastens the malignancy progression by increasing invasion and migration in gastric cancer, head and neck cancer, and glioma cells.⁷ *IFITM1* also appears to be a highly effective

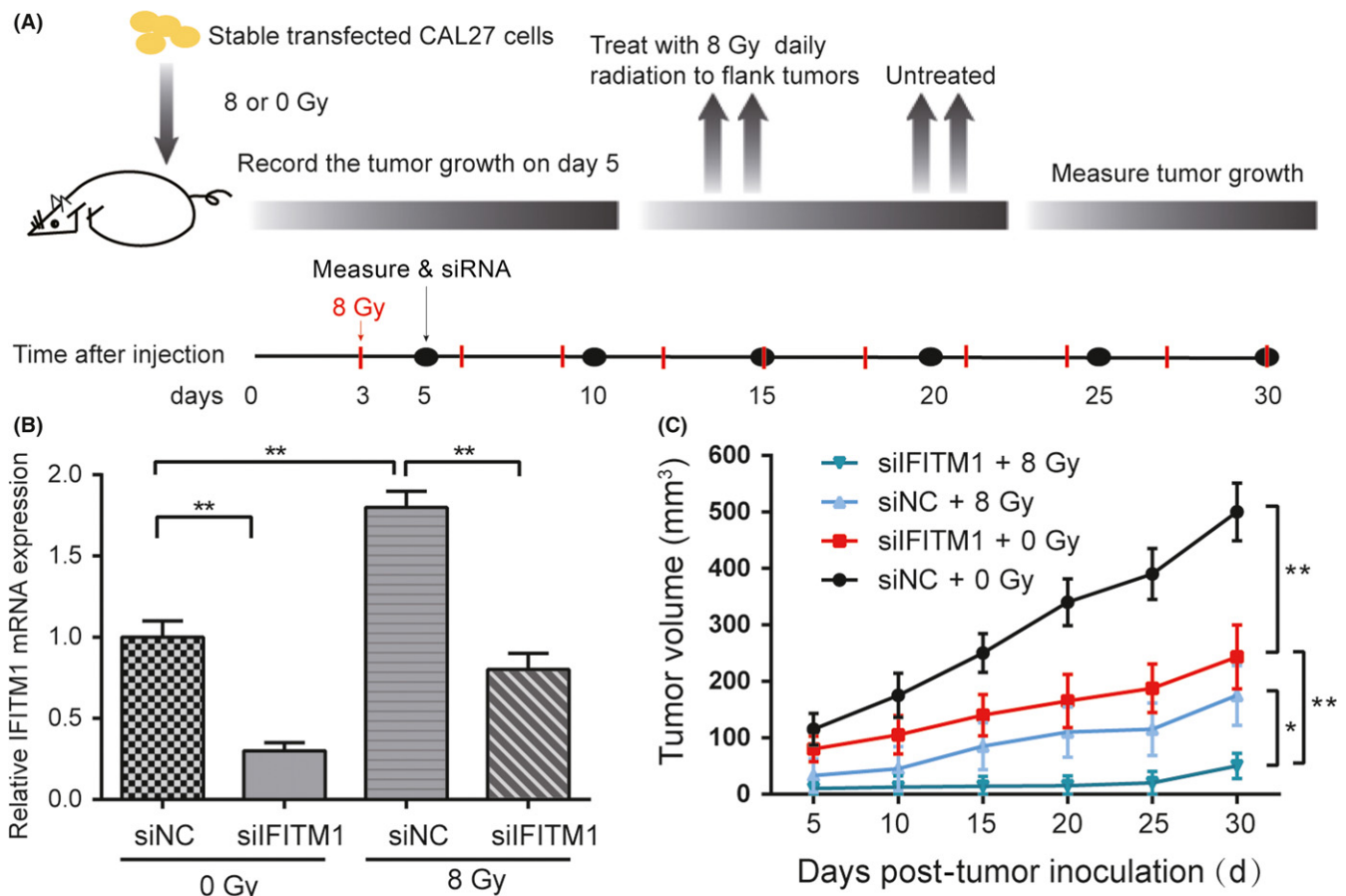


FIGURE 8 *IFITM1* in combination with radiation inhibited oral neoplasm in in vivo tumorigenesis. (A) The experimental process to establish a mouse xenograft tumor model. (B) The expression of *IFITM1* in each group of mice. $**P < 0.01$ meant that there lay significant statistical difference compared to siNC group or 0 Gy. (C) Tumor growth volume curve in each group of mice. Silencing *IFITM1* in combination with radiotherapy group had the smallest tumor growth volume. Results were shown by SD and mean. Significant statistical difference occurred on the basis of $*P < 0.05$ compared to siNC group.

biomarker as its expression has been definitively associated with progression and invasion in several tumors.⁸ More specifically, Lui et al⁹ investigated the effect of *IFITM1* suppression in the proliferation and invasion of aromatase inhibitor-resistant breast cancer in vivo by JAK/STAT-mediated induction of p21. Busca et al¹⁶ suggest that *IFITM1* is superior to CD10 as a marker of endometrial stroma in the evaluation of myometrial invasion by endometrioid adenocarcinoma. Ramanathan⁸ also report *IFITM1* gene expression as a biomarker for the early detection of invasive oral squamous cell carcinomas.

Multi-fraction radiation treatment is advantageous in tumor control because: (a) greater nonrepairable damage is induced per unit dose in tumor cells; (b) tumor reoxygenation can occur between each fraction; and (c) the redistribution of clonogenic tumor cells into more radiosensitive portions of the cell cycle can transpire as treatment progresses. Cell survival assays, which are widely used in radiobiology research, have provided useful information regarding cells that do not die rapidly following radiation exposure.³ For instance, we now know that the *IFITM1* gene can be increased by radiation in a wide variety of tumor cell lines³ and that it can regulate human cell proliferation after X-ray treatment.¹⁷

Our results demonstrated the relationship between *IFITM1* and radiation in the treatment of oral neoplasm. From the results, there is no doubt that the treatment of si-*IFITM1* combined with radiotherapy was the best method for oral neoplasm cells. Beyond this study, much research in radiotherapy has been documented in various fields. Take-mura et al¹⁸ used the age-adjusted Charlson comorbidity index to predict the prognosis of laryngopharyngeal cancer patients treated with radiation therapy; Wang et al¹⁹ performed a clinical analysis of recurrence patterns in patients with nasopharyngeal carcinoma treated with intensity-modulated radiotherapy; and Dohm et al²⁰ studied the effect of early or late radiotherapy following gross or subtotal resection for atypical meningiomas.

Although there are some valuable insights in this research, there is no doubt that problems remain. It is apparent that *IFITM1* likely impacts not only oral neoplasm but also many other forms of cancer. It is also the case that radiotherapy has its own disadvantages, many of which are quite harmful. For oral neoplasm, there are still a large amount of issues to be addressed in future research. In this study as a whole, however, the overexpression of *IFITM1* was seen to upgrade cell proliferation and cell apoptosis in CAL27, TSCC1 and KB cells. In contrast, cell proliferation and apoptosis can be inhibited by radiotherapy. As a result, the evidence points to strong support for the combination of radiotherapy with the inhibition of *IFITM1*. Therefore, this study may inform promising avenues for the treatment of oral neoplasm.

CONFLICT OF INTEREST

The authors declare that no potential conflicts of interest exist.

ORCID

Xiaojiang Li  <http://orcid.org/0000-0002-8487-0315>

REFERENCES

1. Smitha T, Mohan CV, Hemavathy S. Prevalence of human papillomavirus16 DNA and p16(INK4a) protein in oral squamous cell carcinoma: a systematic review and meta-analysis. *J Oral Maxillofac Pathol.* 2017;21:76-81.
2. Oghumu S, Casto BC, Ahn-Jarvis J, et al. Inhibition of pro-inflammatory and anti-apoptotic biomarkers during experimental oral cancer chemoprevention by dietary black raspberries. *Front Immunol.* 2017;8:1325.
3. Tsai MH, Cook JA, Chandramouli GV, et al. Gene expression profiling of breast, prostate, and glioma cells following single versus fractionated doses of radiation. *Cancer Res.* 2007;67:3845-3852.
4. Musunuru HB, Davidson M, Cheung P, et al. Predictive parameters of symptomatic hematochezia following 5-fraction gantry-based SABR in prostate cancer. *Int J Radiat Oncol Biol Phys.* 2016;94:1043-1051.
5. Molinier J, Kerr C, Simeon S, et al. Comparison of volumetric-modulated arc therapy and dynamic conformal arc treatment planning for cranial stereotactic radiosurgery. *J Appl Clin Med Phys.* 2016;17:92-101.
6. Coelho RC, Da Silva FML, Do Carmo IML, Bonaccorsi BV, Hahn SM, Faroni LD. Is there a role for salvage radiotherapy in locally advanced breast cancer refractory to neoadjuvant chemotherapy? *Breast.* 2017;31:192-196.
7. He J, Li J, Feng W, Chen L, Yang K. Prognostic significance of IFN-induced transmembrane protein 1 in colorectal cancer. *Int J Clin Exp Pathol.* 2015;8:16007-16013.
8. Ramanathan A, Ramanathan A. Interferon induced transmembrane protein-1 gene expression as a biomarker for early detection of invasive potential of oral squamous cell carcinomas. *Asian Pac J Cancer Prev.* 2016;17:2297-2299.
9. Lui AJ, Geanes ES, Ogony J, et al. IFITM1 suppression blocks proliferation and invasion of aromatase inhibitor-resistant breast cancer in vivo by JAK/STAT-mediated induction of p21. *Cancer Lett.* 2017;399:29-43.
10. Chen Z, Soutto M, Rahman B, et al. Integrated expression analysis identifies transcription networks in mouse and human gastric neoplasia. *Genes Chromosom Cancer.* 2017;56:535-547.
11. Ogony J, Choi HJ, Lui A, Cristofanilli M, Lewis-Wambi J. Interferon-induced transmembrane protein 1 (IFITM1) overexpression enhances the aggressive phenotype of SUM149 inflammatory breast cancer cells in a signal transducer and activator of transcription 2 (STAT2)-dependent manner. *Breast Cancer Res.* 2016;18:25.
12. Zheng W, Zhao Z, Yi X, et al. Down-regulation of IFITM1 and its growth inhibitory role in cervical squamous cell carcinoma. *Cancer Cell Int.* 2017;17:88.
13. Yu F, Xie D, Ng SS, et al. IFITM1 promotes the metastasis of human colorectal cancer via CAV-1. *Cancer Lett.* 2015;368:135-143.
14. Kim NH, Sung HY, Choi EN, et al. Aberrant DNA methylation in the IFITM1 promoter enhances the metastatic phenotype in an intraperitoneal xenograft model of human ovarian cancer. *Oncol Rep.* 2014;31:2139-2146.
15. Fumoto S, Shimokuni T, Tanimoto K, et al. Selection of a novel drug-response predictor in esophageal cancer: a novel screening method using microarray and identification of IFITM1 as a potent marker gene of CDDP response. *Int J Oncol.* 2008;32:413-423.
16. Busca A, Djordjevic B, Giassi A, Parra-Herran C. IFITM1 is superior to CD10 as a marker of endometrial stroma in the evaluation of myometrial invasion by endometrioid adenocarcinoma. *Am J Clin Pathol.* 2016;145:486-496.
17. Kita K, Sugaya S, Zhai L, et al. Involvement of LEU13 in interferon-induced refractoriness of human RSa cells to cell killing by X rays. *Radiat Res.* 2003;160:302-308.

18. Takemura K, Takenaka Y, Ashida N, et al. Age-adjusted Charlson Comorbidity Index predicts prognosis of laryngopharyngeal cancer treated with radiation therapy. *Acta Otolaryngol.* 2017;137:1307-1312.
19. Wang L, Guo Y, Xu J, et al. Clinical analysis of recurrence patterns in patients with nasopharyngeal carcinoma treated with intensity-modulated radiotherapy. *Ann Otol Rhinol Laryngol.* 2017;126:789-797.
20. Dohm A, McTyre ER, Chan MD, et al. Early or late radiotherapy following gross or subtotal resection for atypical meningiomas: clinical outcomes and local control. *J Clin Neurosci.* 2017;46:90-98.

How to cite this article: Yang J, Li L, Xi Y, et al. Combination of *IFITM1* knockdown and radiotherapy inhibits the growth of oral cancer. *Cancer Sci.* 2018;109:3115–3128. <https://doi.org/10.1111/cas.13640>